

Prestress and excitation force identification in a prestressed concrete box-girder bridge

Ziru Xiang*, Tommy H.T. Chan^a, David P. Thambiratnam^a and Andy Nguyen^b

School of Civil Engineering and Built Environment, Queensland University of Technology, George St, Brisbane, Queensland 4000, Australia

(Received July 25, 2017, Revised August 10, 2017, Accepted August 19, 2017)

Abstract. Prestress force identification (PFI) is crucial to maintain the safety of prestressed concrete bridges. A synergic identification method has been proposed recently by the authors that can determine the prestress force (PF) and the excitation force simultaneously in prestressed concrete beams with good accuracy. In this paper, the ability of this method in the application with prestressed concrete box-girder bridges is demonstrated. A reasonable assumption is made to capture the similarity of the dynamic behavior of the prestressed concrete box-girder bridge and a beam under a certain loading scenario, and the feasibility of this method for application in a prestressed box-girder bridge is affirmed. A comprehensive laboratory test program is conducted, and the effects of PF, excitation, measuring time and uncertainties are studied. Results show that the proposed method can predict the PF and the excitation force in a prestressed concrete box-girder accurately and has a great robustness against uncertainties.

Keywords: prestress force identification; moving load identification; synergic identification; virtual distortion method

1. Introduction

At present, prestressed concrete bridges (PCBs) play a significant role in the transport networks globally. However, potential safety hazards are raised through the widely used prestressed concrete bridges. Several bridge failures have been reported due to failures in the prestressing system and have caused large losses, such as the collapse of Koror-Babeldaob Bridge (Bazant *et al.* 2012). Prestressed concrete beams can incur a loss in the prestress force (PF) as a result of elastic shortening, creep and shrink of concrete, steel relaxation and frictional loss between tendon and concrete, which in turn would reduce the strength of the beam, shorten the lifecycle of the bridge or even lead to catastrophic failures. It is hence crucial to monitor the magnitude of the PF in the prestressed concrete beam to ensure that it remains within a safe range.

Unfortunately, PF in an existing PCB is not easy to evaluate. The most basic and easiest way to estimate whether there are PF losses is through visual inspection (Weischedel 1985, Choquet and Miller 1988, Geller and Udd 1992, Weischedel and Hoehle 1995). Generally, in these methods, it is assumed that the prestressed tendons would have lost some of the PF if cracks occur around the tendons, and the presence of visible damage such as kinks, nicks, severed wires, extensive yielding and unraveling to the exposed strands that can lead to a significant loss of the PF. However, it is quite possible that a tendon could exhibit

none of these physical attributes of damage and still loses the PF value seriously. As a result, these visual inspection methods are not reliable in prestress force identification (PFI).

Some studies pointed out that Ultrasonic wave can assess the stress level in prestressed components directly because it reveals substantial subsurface flaws in materials (Lozev *et al.* 1996, Pei and Demachi 2011, Hussin *et al.* 2015). But these studies were limited to laboratory applications, and are time-consuming and sometimes hazardous. Further, the required instruments are costly and often not reliable for long term monitoring.

To overcome limitations in visual inspections and non-destructive testing methods, different indirect identification approaches have been proposed since the middle of the 1990s. The PF could be examined on the basis that the loss of the PF in the structure is related to the change in structural stiffness which can be estimated by monitoring changes in vibration characteristics of the structure (Kim *et al.* 2003).

Some researchers studied the relationship between the PF and modal characteristics and tried to detect PF via natural frequencies of PCBs (Saiidi *et al.* 1994, Dall'asta and Dezi 1996, Miyamoto *et al.* 2000, Materazzi *et al.* 2009, Ni *et al.* 2012). However, these methods faced the issue of insensitivity of modal parameters against PF and their variation tendency changes distinctly through different prestressing techniques: PF introduced by the prestressing tendon reduces the natural frequency of PCB, but the prestressing tendon itself increases the flexural rigidity and hence the natural frequency (Lu and Law 2006). The change of natural frequency depends on these dual effects and hence can be hardly predicted for different cases. These methods were therefore not effective for detecting the existing PF in structures.

*Corresponding author, Ph.D. Student

E-mail: ziru.xiang@hdr.qut.edu.au

^aProfessor

^bPh.D.

More recently, some methods to assess PF inversely were derived using measured dynamic responses such as strains or accelerations (Law and Lu 2005, Lu and Law 2006, Vélez *et al.* 2010, Xu and Sun 2011), but the lack of computational stability and accuracy hindered their wide application. Besides, all these methods require a known exciting force which in practice is inconvenient because bridges need to be closed during testing, otherwise passing vehicles may affect the excitation.

To overcome these problems, a synergic identification method was recently proposed by the authors to determine the PF and the excitation force in a prestressed concrete member simultaneously using its dynamic response (Xiang *et al.* 2015, Xiang *et al.* 2016). Case studies by means of numerical simulations were conducted and the results showed that the proposed method was capable of identifying both the PF and moving force simultaneously while being robust to measurement noise. However, the proposed method was formulated for simply supported beams, while in practice; many PCBs are box-girder bridges. The ability of this method to be applied for prestressed box-girder bridges deserves further validation. Therefore, in this paper, the synergic identification method is extended to estimate the PF and excitation force simultaneously in prestressed concrete box-girder bridge through the dynamic response induced by this excitation. Several modifications are made for the extension including a reasonable assumption on the simulation of the box-girder bridge by two-dimensional beam elements. A comprehensive laboratory test program is then carried out for experimental validation purposes.

2. Method

This section describes the synergic identification method to simultaneously determine the PF and the excitation force. The method is first formulated for a simply supported beam and then extended to a prestressed concrete box-girder bridge with a reasonable assumption.

2.1 Forward problem

The inspiration of this method comes from the Virtual Distortion Method (VDM) that estimates the structural damage and the exciting force (Zhang *et al.* 2012). As PF, similar to structural damage, changes the stiffness of the structure, VDM can be implemented to identify the PF to some extent.

The VDM is a quick reanalysis method conceptually similar to the initial strains approach (Kołakowski *et al.* 2008), which represents the modification in structural response under equivalent pseudo-loads that are applied to its degrees of freedom (DOFs). Thus, the response of the modified structure can be efficiently obtained without a full structural simulation, merely by adding the response caused by these pseudo-loads to the original response. In this way, the PF in a structure can be transformed to pseudo-loads, and the prestressed structure under an excitation can then be considered as the original structure (without PF) subjected to certain pseudo-loads and the same external excitation.

These two structures share the same dynamic responses.

In Finite Element Method (FEM), a prestressed two-dimensional beam element is described as

$$\{P\}_i = \bar{K}_i \{x\}_i \tag{1}$$

$$\bar{K}_i = K_{n,i} - K_{g,i} \tag{2}$$

where $\{P\}_i$ and $\{x\}_i$ are the nodal force and displacement in the local coordinate system, \bar{K}_i is the local stiffness matrix and can be composed of $K_{n,i}$ and $K_{g,i}$, which are respectively the local stiffness matrix of a normal beam element without PF and the geometrical stiffness matrix containing the information of PF (Lu and Law 2006). Therefore, the local nodal force in Eq. (1) can be represented by the nodal force $\{P\}_i^n$ of original structure element (normal beam element without PF) and the nodal force $\{P\}_i^e$ relevant to the geometrical stiffness matrix (shown in Eq. (3)), which in this paper is called the local pseudo-load. The pseudo-load is presented in Eq. (4) in which T is the PF amplitude and η is the length of the element.

$$\{P\}_i = \{P\}_i^n + \{P\}_i^e \tag{3}$$

$$\{P\}_i^e = K_{g,i} \{x\}_i = \frac{T}{30\eta} \begin{bmatrix} 30 & 0 & 0 & -30 & 0 & 0 \\ 0 & 36 & 3\eta & 0 & -36 & 3\eta \\ 0 & 3\eta & 4\eta^2 & 0 & -3\eta & -\eta^2 \\ -30 & 0 & 0 & 30 & 0 & 0 \\ 0 & -36 & -3\eta & 0 & 36 & -3\eta \\ 0 & 3\eta & -\eta^2 & 0 & -3\eta & 4\eta^2 \end{bmatrix} \{x\}_i \tag{4}$$

In VDM, the local pseudo-load modifies the element in the form of virtual forces. And all these forces follow the modified element's own vibrational behaviour, which means the virtual forces will act exactly the same way as the nodal forces of the element (Xiang *et al.* 2016). In this case, there are three components of virtual distortions, which correspond to the three states of deformation. Based on the orthogonal analysis, the deformation states: axial distortion, pure bending, and bending plus shear terms are obtained through the solution of the Eigenproblem of the element stiffness matrix (Zhang *et al.* 2010). Relevantly, there are three components of virtual forces: the axial force, shear force and bending moment. In addition, we should note that these three forces do not exist perpetually but occur depending on the vibration situation.

Thus, the local pseudo-load can be written as a combination of its virtual forces applied to each element, where $\{p\}_{ik}^e$ is the k^{th} virtual force caused by the i^{th} virtual distortion.

$$\{P\}_i^e = \sum_k \{p\}_{ik}^e \tag{5}$$

In the case of this paper, the simply supported beam is subjected to a vertical excitation as shown in Fig. 1. Thus, only shear force and bending moment are produced, $k=2$.

Assembling the virtual forces in global coordinates, the global pseudo-load $\{P\}$ containing the PF can be calculated

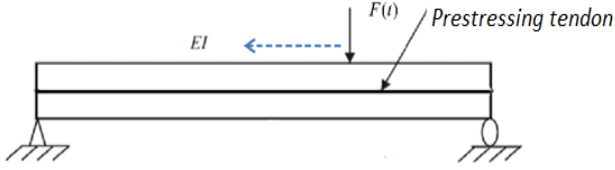


Fig. 1 Simply supported prestressed concrete beam model

by global displacement $\{x\}$ of the prestressed structure which is measurable.

$$\{P\} = \frac{T}{30\eta} \begin{bmatrix} 30 & 0 & 0 & -30 & 0 & 0 & \cdot & \cdot & \cdot \\ 0 & 36 & 3\eta & 0 & -36 & 3\eta & \cdot & \cdot & \cdot \\ 0 & 3\eta & 4\eta^2 & 0 & -3\eta & -\eta^2 & \cdot & \cdot & \cdot \\ -30 & 0 & 0 & 30 & 0 & 0 & -30 & 0 & 0 \\ 0 & -36 & -3\eta & 0 & 72 & 0 & 0 & -36 & 3\eta \\ 0 & 3\eta & -\eta^2 & 0 & 0 & 8\eta^2 & 0 & -3\eta & -\eta^2 \\ \cdot & \cdot & \cdot & -30 & 0 & 0 & 30 & 0 & 0 \\ \cdot & \cdot & \cdot & 0 & -36 & -3\eta & 0 & 36 & -3\eta \\ \cdot & \cdot & \cdot & 0 & 3\eta & -\eta^2 & 0 & -3\eta & 4\eta^2 \\ \cdot & \cdot \end{bmatrix} \{x\} \quad (6)$$

It should be mentioned that T is a time-dependent variable because both of the matrixes in Eq. (6) have the dimension of time. Therefore, theoretically, a successful identification will produce a time history of T , which can then be averaged to give the final identified values of PF.

Therefore, for a simply supported prestressed beam subjected to a moving force as shown in Fig. 1, the equation of motion, Eq. (6) is rewritten to the equation of non-prestressed beam subjected to the excitation force (moving load) and global pseudo-load Eq. (7).

$$M\{\ddot{x}\} + C\{\dot{x}\} + \bar{K}\{x\} = B\{f\} \quad (7)$$

$$M\{\ddot{x}\} + C\{\dot{x}\} + K\{x\} = B\{f\} + \{P\} \quad (8)$$

where $\{x\}$, $\{\dot{x}\}$ and $\{\ddot{x}\}$ are the displacement, velocity and acceleration vectors, respectively; M , C and \bar{K} are the mass, damping and global stiffness matrices of the prestressed girder, respectively; $\{f\}$ is the excitation force vector, while B is its mapping matrix; K is the global stiffness matrix of the beam without PF (i.e., the original structure).

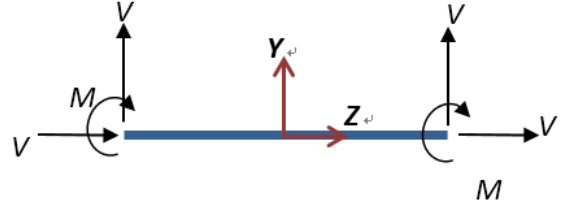
The synergic identification of excitation force and PF, therefore, turns into the identification of the excitation force and the global pseudo-load, and the global pseudo-load is presented in the form of local virtual forces in each node.

2.2 Inverse problem

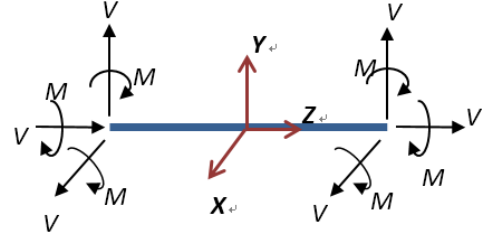
With the assumption of zero initial conditions, the dynamic response is obtained by the convolution of all external forces and their impulse response functions. The matrix form of Duhamel integral is shown as follows,

$$Y_j = H^j F + \sum_k \sum_i^n D_{ik}^j P_{ik} \quad j=1,2,3...nk+1 \quad (9)$$

where Y_j is the discrete response measured by the j^{th} sensor. F and P_{ik} are the discrete excitation load and virtual force



(a) 2D 3 degrees of freedom beam element



(b) 3D 6 degrees of freedom beam element

Fig. 2 Different beam element geometry

vector respectively. n is the element number of the beam. H^j and D_{ik} are matrices composed of impulse response functions between the j^{th} sensor with F and P_{ik} respectively. Based on the definition of Duhamel integral, the impulse response functions are obtained by the Dirac delta functions acted upon the positions of the real forces and hence distinguish these different forces. Therefore, this method requires awareness of the application points of the unknown loads in advance. In order to have a unique solution of this matrix, the responses should not be lesser than the number of the unknowns, which means the number of the sensors should be equal to at least $nk+1$.

During the inversion of Eq. (9), the ill-conditioned problem will occur because of the singularity of the system matrix. Moreover, it is computational costly in the cases of long sampling duration or dense time discretization. Typical regularization solutions for the ill-conditioned problem are the truncated singular value decomposition (TSVD) and Tikhonov method (Jacquelin *et al.* 2003), but it requires additional works.

The authors have already introduced the Load shape-function (LSF) in previous research and efficiently overcame these drawbacks without causing additional computational effort (Xiang *et al.* 2016).

LSF is a fitting approach which treats the load as a ‘beam’ and simulates load record by the shape-function of beam element as Eq. (10).

$$F = N\alpha \quad (10)$$

where N is the LSF matrix and α is its relevant coefficient. Because the number of columns in N is far less than number of rows, it makes α much smaller in dimension than F . The calculation effort of Eq. (9) is therefore reduced. In addition, because the estimated load is smoothed via LSF to some degree, the influence of noise will be minimized even without regularization (Zhang *et al.* 2008). The enhanced Duhamel integral is

$$Y_j = H^j N\alpha_F + \sum_k \sum_i^n D_{ik}^j N\alpha_{ik} = B_F^j \alpha_F + \sum_k \sum_i^n B_{ik}^j \alpha_{ik} \quad (11)$$

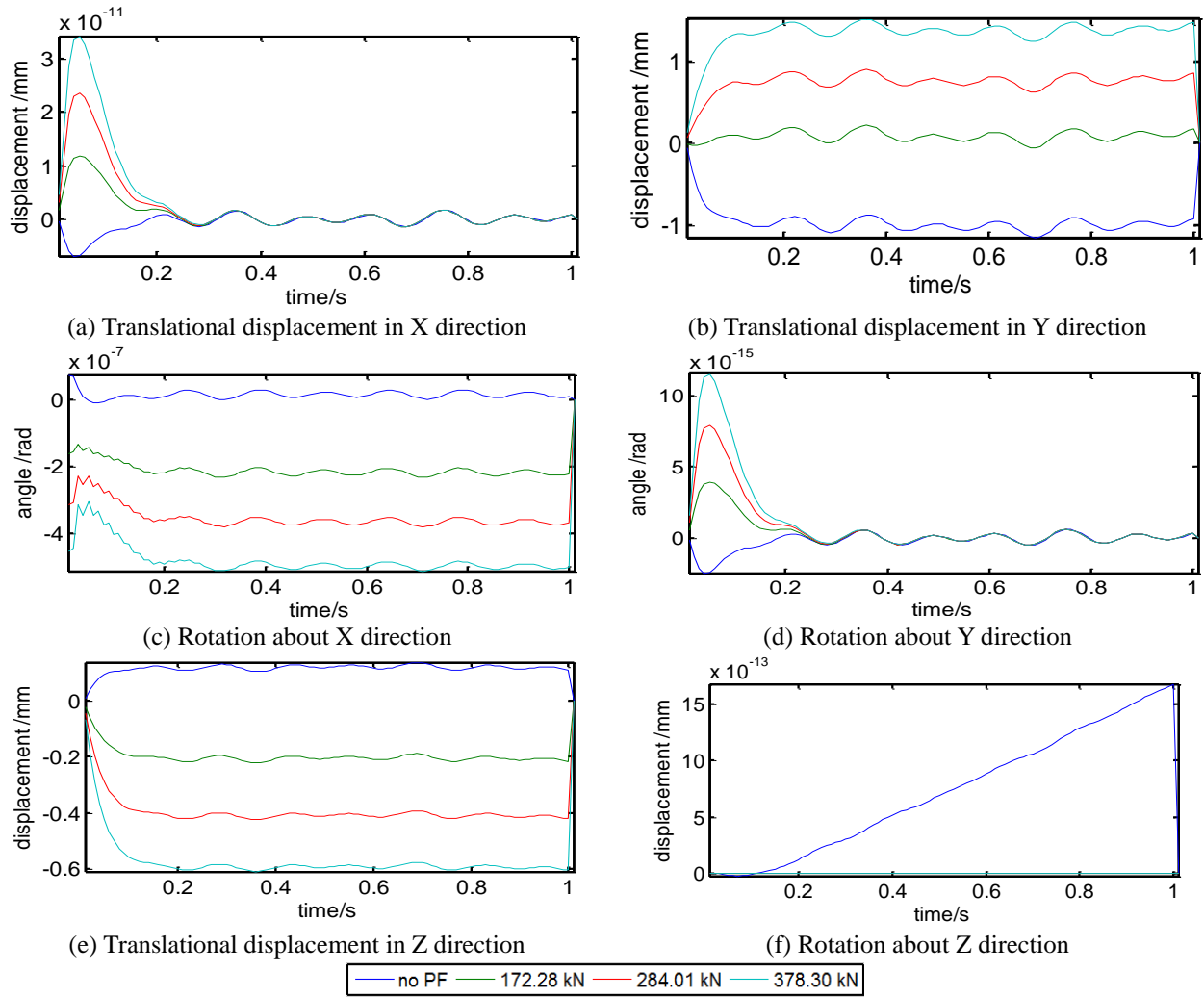


Fig. 3 Displacement responses of prestressed box-girder bridge

where α_F is the relevant coefficient of the moving load and α_{ik} is the coefficient for the k th virtual force caused by the i th local pseudo-load.

Therefore, the excitation force and local virtual force can be identified by solving

$$\begin{bmatrix} \alpha_F \\ \alpha_{11} \\ \vdots \\ \alpha_{kN} \end{bmatrix} = \begin{bmatrix} B_F^1 & B_{11}^1 & \cdots & B_{kN}^1 \\ \vdots & \vdots & & \\ \vdots & \vdots & & \\ \vdots & \vdots & & \\ B_{kN}^{kN+1} & & & B_{kN}^{kN+1} \end{bmatrix}^+ \begin{bmatrix} Y_1 \\ Y_2 \\ \vdots \\ Y_{kN+1} \end{bmatrix} \quad (12)$$

$$F = N\alpha_F \quad (13)$$

$$P_{ik} = N\alpha_{ik} \quad (14)$$

At last, PF is determined in the global coordinate through Eq. (6).

2.3 Application to prestressed box-girder bridge

As there is no specific theory for box-girders, researchers usually use beam or plate based theories to

approach the vibration of box-girders. As mentioned earlier, the synergic identification method has already been developed for a 2D simply supported beam; it is extended for the application in box-girder bridges by changing the cross section of the rectangular girder to a box-girder. Several significant differences are generated by this change. As box-girder is a 3D structure, 3D beam element should be introduced in the FE analysis. Compared to the 2D three degrees of freedom beam element used in the 2D beam which contains translational displacements in the Y and Z directions as well as the rotation in X direction, the 3D beam element has six degrees of freedom which is a translational displacement and a rotation in and about the directions of X, Y and Z respectively. Relevantly, the nodal forces in each node of this element are the shear forces and moments in the three directions respectively (as shown in Fig. 2).

This difference influences the implement of VDM. As we know, the pseudo-load is represented as virtual forces at each node, and the virtual forces follow the same form of the real nodal forces. Therefore, the pseudo-load in the model of prestressed concrete box-girder bridge is composed of the virtual forces in the directions of X, Y, and Z, the k in Eq. (5) equals to 6, which increases the computational work dramatically at the same time.

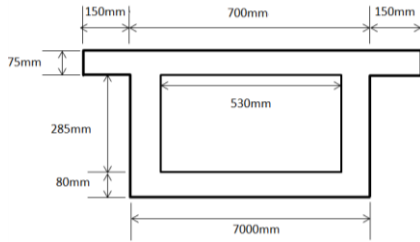


Fig. 4 Cross-section of the model

Table 1 Prestressing tendon arrangement

Longitude (mm)	0	500	1000	1500	2000	2500	3000
Distance (mm)	235	209	184	163	146	134	130

To overcome this problem, an investigation is conducted to compare the displacement responses at several points along the central axial axes of the box-girder bridge with different levels of PFs subjected to an excitation force (by means of simulation). From the displacement of the center of mid-span shown in Fig. 3, it is found that the translational displacements in the directions of X and Z are far less than that in direction Y. The same also happens for the rotations in about the direction of X and Y in comparison with that about the Z direction. Moreover, the change in PF causes no difference in the translational displacement in the X direction and very small difference in the Z direction, while the change in PF results in almost no difference in the rotations about the Y and Z directions (same situations occur at other points). This shows that under the present loading scenario, the dynamic behaviour of the nodes along the central axis of the box-girder bridge is similar to that in a two-dimensional beam, and the influence of PF is mainly reflected in the translational displacement in the Y direction and rotation about the X direction which are also similar to the two-dimensional beam element. Therefore, it is reasonable to assume that we can use the virtual forces in 2D beam element to approximately simulate the points along the central axis of the box-girder bridge. And under the loading scenario of vertical excitation force, the nodal forces of these 2D beam elements are assumed to be translational displacement in the Y direction and rotational angel around the X direction, which means in Eq. (5), k equals to 2.

In the aspect of LSF implemented Duhamel integral, the integral can be applied to all linear system; there is no difference between the 2D beam and 3D box-girder bridge as long as the girder is considered as being linear.

In conclusion, the synergic identification is promising in the application of prestressed concrete box-girder bridge. The potential will be experimentally verified in the next section.

3. Laboratory test

3.1 The prestressed box-girder bridge details

A 6-meter-long single cell box-girder bridge whose

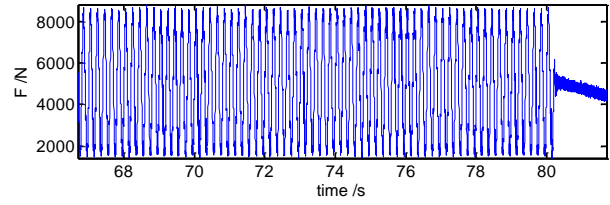


Fig. 5 Excitation load record

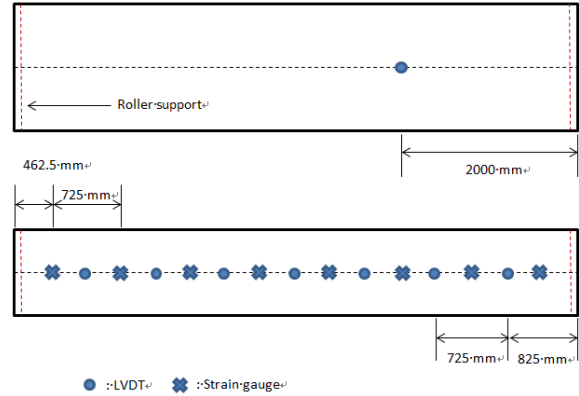


Fig. 6 Sensor arrangement

Table 2 Case setting

Case No.	PF (kN)	Measuring time (s)	Response record No.
1	171.277	3	1.1
2	284.009	3	2.1
3	284.009	10	2.2
4	378.293	3	3.1
5	378.293	10	3.1

cross-section is described in Fig. 4 was constructed in the laboratory. Two unbounded tendons each of 15.2 mm diameter were utilized in the box-girder bridge with each tendon embedded into the concrete through a 20 mm diameter duct in order to apply different levels of PFs by a hydraulic mono jack. The tendon profile was selected as parabolic with eccentricity; the distance of the tendon to the bottom slab along the longitudinal direction is shown in Table 1.

Grade 32 concrete was selected to construct the box-girder. Sufficient longitudinal and shear reinforcements were provided; the longitudinal steel bar ratio and lateral steel bar ratio were 0.01134 and 0.01161 respectively.

3.2 Case setting

The prestressed box-girder bridge model was excited by a sinusoidal force applied to the center of mid-span. The loading period is around 100 s, which is partly shown in Fig. 5. The synergic method was validated in this test for 3 levels of PF. Vertical displacements and longitudinal strain responses were measured from the test at a sampling rate of 2000 Hz. The sensor arrangement is shown in Fig. 6, with all the sensors installed along the bottom central axis along the longitudinal direction of the bridge according to the

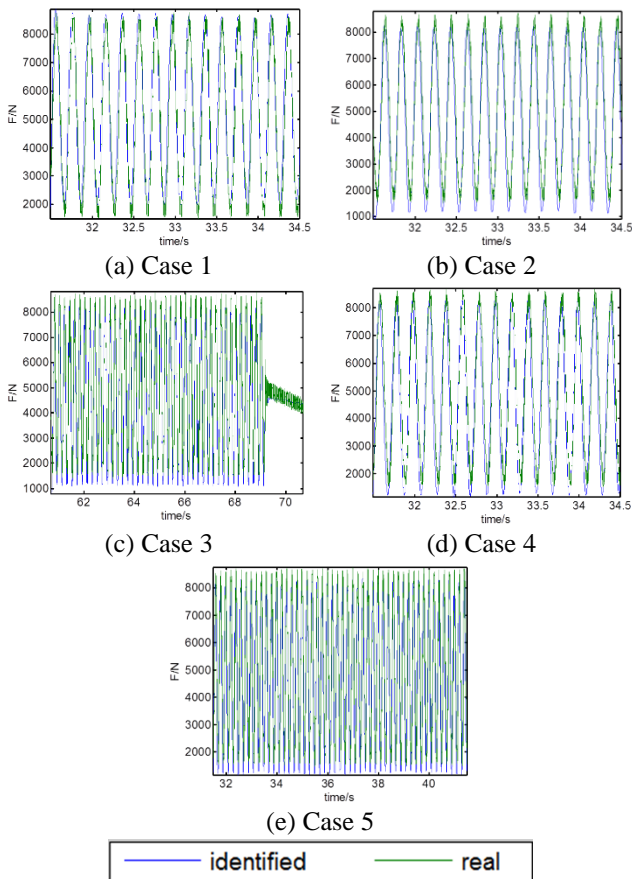


Fig. 7 Excitation identification results

proposed assumption. The impulse response and dynamic influence matrixes were formulated by the updated FE model.

During the dynamic test, the excitation was applied twice at each stage of PF. Thus 5 series of response records including displacements and strains are measured, which are numbered by the PF level and test sequence, for example, the response record measured in the first test of first PF level is 1.1. Considering the variation of measuring time, a difference of excitation (excitation forces generated by the loading frame have slight difference each time), and changes of PF amplitude, the case setting is listed in Table 2. Note that for the sake of clarity and to be representative, the time periods are selected starting from 31.5 s (Case 1, 2, 4 and 5) or 61 s (Case 3).

3.3 Results and discussion

In this section, synergic identification results of all cases are discussed. Excitation estimation and PF prediction are shown separately. The impact of measuring time, excitation force and PF amplitude in this method are studied.

In Fig. 7, excitation force identification results are presented, which show very good agreement with the actual force except for some small errors at peaks. Moreover, small fluctuations in factual force records are smoothed in the results, as the measurement noise as well as the minor waves has been eliminated by using LSF. Thus, it is predicted that this method has a great robustness to

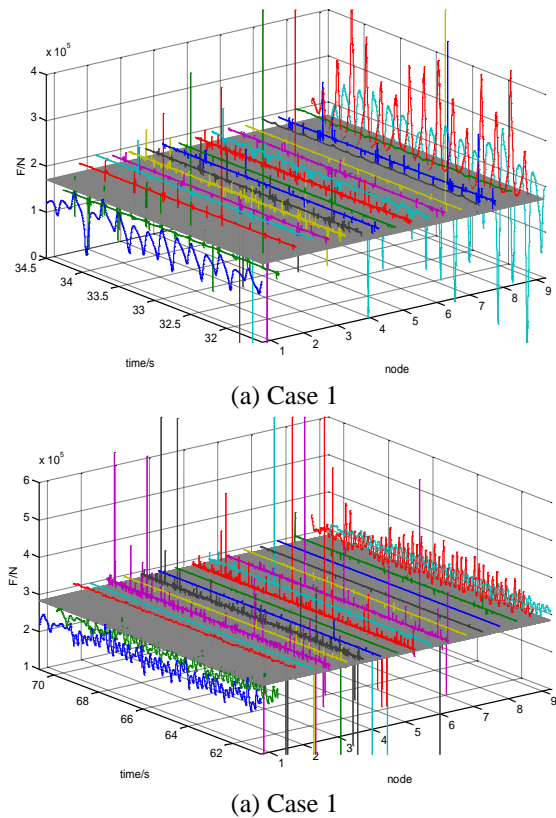


Fig. 8 Overall PFI results in Cases 1 and 3

Table 3 Average of T function in each node

Node	Case 1	Case 2	Case 3	Case 4	Case 5
2	181.49	311.21	310.80	391.06	391.16
	190.01	300.04	299.91	397.82	399.92
3	180.64	298.85	299.02	391.13	391.05
	181.19	297.12	297.26	390.78	391.25
4	178.63	294.12	294.03	389.07	389.09
	180.71	291.66	291.72	390.73	390.71
5	174.77	290.06	289.86	384.87	384.85
	179.15	288.88	289.11	388.93	389.07
6	180.35	292.51	292.45	391.20	391.21
	181.08	291.03	291.03	391.34	391.22
7	180.51	297.36	297.31	390.39	390.40
	185.48	295.18	295.04	394.83	395.12
8	181.26	299.56	299.56	391.61	391.58
	192.60	299.67	302.90	402.79	402.96
Average	182.00	296.23	296.43	391.90	392.11
True	171.28		284.01		378.29
Error	6.25%	4.30%	4.37%	3.59%	3.65%

*Values in each cell are listed as PF identified by virtual shear force and by virtual moment

measurement noise.

In addition, from Fig. 7(c) showing Case 3, the linear decrease force, as well as the sinusoidal force is also identified precisely. The capability of this method to determine different types of forces is hence validated.

The overall identified PFs in Cases 1 and 3 are selected to demonstrate in Fig. 8. The T functions which represent the PF values are calculated from global virtual forces in 9 nodes via Eq. (5), thus 18 results (8 from vertical

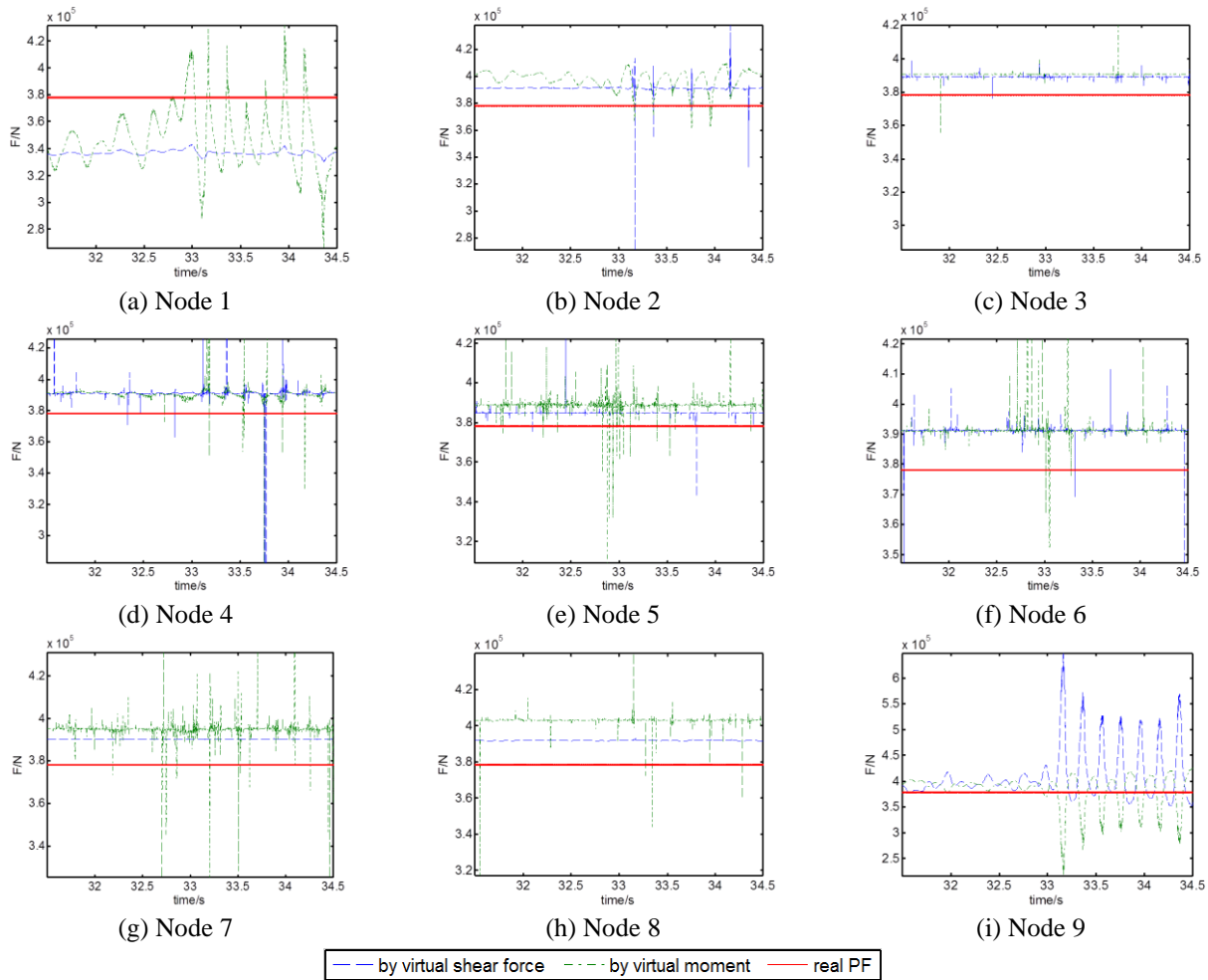


Fig. 9 PFI results of each node in Case 4

displacements and 8 from rotations) are shown in each picture.

The results of each node in Case 4 are demonstrated in Fig. 9 for clarity. These T functions have then been averaged to give the final identified values of PF and listed in Table 3.

In Table 3, the nodes at supports have been removed as they obviously cannot provide the true value. The results show that the PF values of all cases are determined with good accuracy; errors are limited to 6.25%.

• Influence of different PF levels

Fig. 8 shows the PFI results obtained at different nodes, PF in each node is demonstrated not by a constant T (shown in Eq. (6)) but as a time-related T function, which has been predicted in section 2.1. It is easy to see that the T functions indicate the PF value at different levels clearly even with some fluctuations, which confirms that the proposed procedure works well for box-girder bridges. This is possible with an identification error limited to around 6%, when the responses along the central longitudinal axes are measured and virtual forces are considered as vertical nodal forces and bending moment similar to 2D beam elements. The identification results are more accurate in the nodes close to mid-span, while the results of nodes at support are subjected to larger error. The reason causing this error is that the dynamic influence matrix is formulated from the FE

model assumed as simply supported (the translational displacements at supports are restrained as 0) while the laboratory model (and also real structures in practice) might not be fully simply-supported and the vertical displacements at supports might therefore not be zero. In terms of the magnitude of the PF, we find that a higher PF value is predicted more accurately, because the virtual forces contribute a bigger proportion to the response and are easier to determine. When the PF is increased from 178.28 kN to 378.29 kN, the error is reduced from 6.25% to 3.65%. Nevertheless, the difference is not large, and according to the authors' previous paper (Xiang *et al.* 2016), the error should be considered acceptable for the practical range of PF value.

• Influence of excitation

In the comparison of Case 2 and 3, the changes in excitation force such as the minor difference in the amplitude and the variation in trend (Case 3 includes the sinusoidal and linear period) have no significant impact on the PFI; only a 0.07% difference is obtained between the errors of these two cases. It means that the excitation has no significant influence on PFI.

• Influence of measuring time

Cases 4 and 5 with the measuring times of 3s and 10s successfully predict the PF, and the error of longer measuring time is slightly higher than the error of shorter

time. This results from the measurement noise; larger errors are introduced to the results with the increase of time duration. However, the inaccuracy is minor as 0.06%; the method is therefore proved to be useful for the synergic identification of PF and static excitation in very short time duration.

- Influence of other uncertainties

In addition, large fluctuations are observed in T function, which resulted from measurement noise and system uncertainties; and the impact tends to be larger at the location of mid-span node (node 5) where excitation applied. This symptom is reasonable as virtual force and excitation act in this node simultaneously and have greater effect on each other. However, due to the enhancement of LSF, the error only leads to some roughness of the T function as expected, which is acceptable and can be further eliminated by some signal processing strategies such as data averaging (i.e., calculating the mean value).

Observing the T functions calculated from the virtual shear force and virtual moment of each node in Fig. 9, we can also find that most of the time the functions from virtual shear force have better performance than from virtual moment. This can be attributed to the identification accuracy of virtual force and moment. As rotation at the node is more difficult to be measured practically, the nodal angles in this experiment are calculated from vertical response data, which is obviously subject to larger error. However, after averaging values in Table 3, the final PFI results calculated by virtual moments are improved and have no serious impact on the accuracy.

4. Conclusions

In this paper, the synergic identification method is extended successfully to determine the PF and excitation in a prestressed concrete box-girder bridge, with the proposed assumption which confirms the box-girder bridge can be approximately simulated by two-dimensional beam elements for a certain loading scenario. A comprehensive laboratory test has been conducted with considerations of the PF amplitude, excitation type, measuring time and uncertainties. Results show that the method can successfully determine the two unknown forces with an error less than 6.25%. In excitation identification, both sinusoidal and linear forces are both determined successfully. On the other hand, with the PFI, changes in the PF and excitation, as well as the measuring time have almost no impact on the accuracy; while the measuring uncertainties form the most significant influence factor, which causes large local fluctuations to the T function, especially to the ones calculated by virtual moments. However, the identification error has been shown to be alleviated through applying common signal processing techniques such as data averaging.

References

Bazant, Z.P., Yu, Q. and Li, G.H. (2012), "Excessive long-time deflections of prestressed box girders. I: Record-span bridge in

- palau and other paradigms", *J. Struct. Eng.*, **138**(6), 676-686.
- Choquet, P. and Miller, F. (1988), "Development and field testing of a tension measuring gauge for cable bolts used as ground support", *CIM Bullet.*, **81**(914), 53-59.
- Dall'asta, A. and Dezi, L. (1996), "Discussion of "prestress force effect on vibration frequency of concrete bridges", *J. Struct. Eng.*, **122**, 458-458.
- Geller, L. and Udd, J. (1992), "NDT of wire ropes with E/M instruments: An examination of operational conditions in Canada", *CIM Bullet.*, **85**(964), 60-67.
- Hussin, M., Chan, T.H., Fawzia, S. and Ghasemi, N. (2015), "Finite element modelling of lamb wave propagation in prestress concrete and effect of the prestress force on the wave's characteristic".
- Jacquelin, E., Bennani, A. and Hamelin, P. (2003), "Force reconstruction: Analysis and regularization of a deconvolution problem", *J. Sound Vibr.*, **265**(1), 81-107.
- Kim, J.T., Ryu, Y.S. and Yun, C.B. (2003), "Vibration-based method to detect prestress loss in beam-type bridges", *Smart Struct. Mater.*, **5057**(1), 55-568.
- Kořakowski, P., Wikłó, M. and Holnicki-Szulc, J. (2008), "The virtual distortion method-a versatile reanalysis tool for structures and systems", *Struct. Multidiscipl. Optim.*, **36**(3), 217-234.
- Law, S.S. and Lu, Z. (2005), "Time domain responses of a prestressed beam and prestress identification", *J. Sound Vibr.*, **288**(4), 1011-1025.
- Lozez, M.G., Clark, A.V. and Fuchs, P.A. (1996), *Application of Electromagnetic-Acoustic Transducers for Nondestructive Evaluation of Stresses in Steel Bridge Structures*.
- Lu, Z. and Law, S.S. (2006), "Identification of prestress force from measured structural responses", *Mech. Syst. Sign. Proc.*, **20**(8), 2186-2199.
- Materazzi, A., Breccolotti, M., Ubertini, F. and Venanzi, I. (2009), "Experimental modal analysis for assessing prestress force in PC bridges: A sensitivity study", *Proceedings of the 3rd International Operational Modal Analysis Conference*.
- Miyamoto, A., Tei, K., Nakamura, H. and Bull, J.W. (2000), "Behavior of prestressed beam strengthened with external tendons", *J. Struct. Eng.*, **126**(9), 1033-1044.
- Ni, Y.Q., Kim, J.T., Ho, D.D., Kim, J.T., Stubbs, N. and Park, W.S. (2012), "Prestress-force estimation in PSC girder using modal parameters and system identification", *Adv. Struct. Eng.*, **15**(6), 997-1012.
- Pei, C. and Demachi, K. (2011), "Numerical simulation of residual stress measurement with acoustic wave", *E-J. Adv. Mainten.*, **2**, 160-167.
- Saïidi, M., Douglas, B. and Feng, S. (1994), "Prestress force effect on vibration frequency of concrete bridges", *J. Struct. Eng.*, **120**(7), 2233-2241.
- Vélez, W., Cruz, A. and Thomson, P. (2010), "Identification of prestress forces using genetic algorithms and generic element matrices", *Proceedings of the AIP Conference*, **1281**(1), 1223-1227.
- Weischedel, H.R. (1985), "The inspection of wire ropes in service: A critical review", *Mater. Eval.*, **43**(13), 1592-1594.
- Weischedel, H.R. and Hoehle, H.W. (1995), "Quantitative nondestructive in-service evaluation of stay cables of cable-stayed bridges: Methods and practical experience", *Nondestr. Eval. Aging Infrastr.*
- Xiang, Z., Chan, T., Thambiratnam, D. and Nguyen, T. (2015), "Prestress force and moving load identification on prestressed concrete beam based on virtual distortion method", *Proceedings of the World Congress on Advances in Structural Engineering and Mechanics*.
- Xiang, Z., Chan, T.H., Thambiratnam, D.P. and Nguyen, T. (2016), "Synergic identification of prestress force and moving load on

- prestressed concrete beam based on virtual distortion method”, *Smart Struct. Syst.*, **17**(6), 917-933.
- Xu, J. and Sun, Z. (2011), “Prestress force identification for eccentrically prestressed concrete beam from beam vibration response”, *Struct. Long.*, **5**(2), 107-115.
- Zhang, Q., Jankowski, Ł. and Duan, Z. (2008), “Identification of coexistent load and damage based on virtual distortion method”, *Proceedings of the 4th European Workshop on Structural Health Monitoring*, Kraków, Poland.
- Zhang, Q., Jankowski, Ł. and Duan, Z. (2010), “Simultaneous identification of moving masses and structural damage”, *Struct. Multidiscipl. Optim.*, **42**(6), 907-922.
- Zhang, Q., Jankowski, Ł. and Duan, Z. (2012), “Simultaneous identification of excitation time histories and parametrized structural damages”, *Mech. Syst. Sign. Proc.*, **33**, 56-68.

HK